Catal Lett (2009) 129:240–246
DOI 10.1007/s10562-008-9807-8

Perovskite-Like Mixed Oxides ($LaSrMn_{1-x}Ni_xO_{4+\delta}$, $0 \leq x \leq 1$) as Catalyst for Catalytic NO Decomposition: TPD and TPR Studies

Junjiang Zhu · Dehai Xiao · Jing Li · Xiangguang Yang

Received: 30 October 2008 / Accepted: 29 November 2008 / Published online: 9 January 2009

Abstract Catalytic NO decomposition on $LaSrMn_{1-x}Ni_xO_{4+\delta}$ ($0 \leq x \leq 1$) is investigated. The activity of NO decomposition increases dramatically after the substitution of Ni for Mn, but decreases when Mn is completely replaced by Ni ($x = 1.0$). The optimum value is at $x = 0.8$. These indicate that the catalytic performance of the samples is contributed by the synergistic effect of Mn and Ni. O_2-TPD and H_2-TPR experiments are carried out to explain the change of activity. The former indicates that only when oxygen vacancy is created, could the catalyst show enhanced activity for NO decomposition; the latter suggests that the best activity is obtained from catalyst with the most matched redox potentials (in this work, the biggest ΔT and ΔE values). The close relationships between activity and ΔT or ΔE indicate that ΔT and ΔE are important parameters of catalyst for NO decomposition.

Keywords Manganese · Nickel · NO decomposition · Perovskite-like oxides · O_2-TPD · H_2-TPR

1 Introduction

Nitrogen oxides (NO_x) formed during various combustion processes force serious damage both to human beings and to environment, such as smog in the urban areas, acidic depositions, stratospheric ozone depletion, etc., [1, 2]. The removal of NO_x from all exhausts remains a great challenge in spite of all progress made over the years [3]. Currently, two technologies are proposed for NO removal in catalysis, as NO decomposition and NO reduction. Catalytic NO decomposition is the most desirable way of removing NO_x from exhaust gas streams since it does not involve the addition of a supplemental reductant and the products (N_2 and O_2) are nontoxic [4, 5], and hence it receives special interest to the catalysis scientists, although no practical application has been reported up to date.

Perovskite-like mixed oxides (A_2BO_4), as well as perovskites (ABO_3), have a well-defined bulk structure and the composition of cations at both A- and B-sites can be changed without destroying the matrix structure [2]. They thus provide an opportunity to control the oxidative state of transition metal(s) and the amount of non-stoichiometric oxygen by partial substitution of the A- and/or B-site cations, and therefore are suitable materials for studying the structure-property relationships of catalyst. Among them, the Mn-based samples are unique, as they are oxygen rich, i.e., $\delta > 0$ [6]. To force the Mn-based samples to become oxygen deficient, another B-site cation can be substituted for manganese, e.g., nickel. [7–9].

Catalytic properties of perovskite-type oxides with ABO_3 or A_2BO_4 structure have been studied extensively. Teraoka et al. [10] demonstrated that the performance of poorly active manganites could be enhanced by partial substitution with other transition metal ions, particularly with nickel. Zhu et al. [11] showed that a new site (Ce^{3+}–(O)–(Ni^{2+}–[]–Ni^{3+}) facilitating oxygen desorption could be formed when La is substituted by Ce in $La_{1-x}Ce_xSrNiO_4$, due to the alterable valence of Ce. They also reported that the catalytic activity of NO decomposition has a close

J. Zhu (✉) · D. Xiao · J. Li · X. Yang
Laboratory of Green Chemistry and Process, Changchun Institute of Applied Chemistry, Chinese Academy of Sciences, 130022 Changchun, China
e-mail: ciaczjj@gmail.com

J. Zhu
Laboratory of Catalysis and Materials, Department of Chemical Engineering, Faculty of Engineering, University of Porto, 4200-465 Porto, Portugal

relation to the redox properties of the catalyst, and the more the match of the redox potentials, the more the activity of the catalyst [12].

In this work, O_2-TPD and H_2-TPR measurements are employed as two major characteristic means for correlating the solid-state properties with the catalytic performance, since O_2-TPD experiment is known as an effective method to investigate the reactivity on catalyst surface, while H_2-TPR is widely used to characterize the redox properties of catalysts, both of which have important implications regarding the catalytic performance. $LaSrMn_{1-x}Ni_xO_{4+\delta}$ ($0 \leq x \leq 1$) with A_2BO_4 structure is used as the catalyst model, since the Mn- and Ni-contained perovskite type oxides are reported to be very active for NO removal [7, 13–16].

2 Experimental

2.1 Preparation

$LaSrMn_{1-x}Ni_xO_{4+\delta}$ ($0 \leq x \leq 1$) was prepared by citrate combustion method as described elsewhere [17]. Briefly, an aqueous solution of La^{3+}, Sr^{2+}, Ni^{2+} and Mn^{2+} nitrates (all AR purity grade) with appropriate stoichiometry was added to a solution of citric acid 100% in excess of stoichiometry. The resulting solution was evaporated to dryness, and then the precursors obtained were decomposed in air at 573 K, calcined at 873 K for 1 h and finally pelletized and calcined at 1,173 K in air for 6 h, the synthesized pellets were pulverized to ca. 40–80 mesh sizes for use.

2.2 Characterization

Powder X-ray diffraction (XRD) data were obtained with an X-ray diffractometer (type D/max-IIB, Rigaku) operated at 40 kV and 10 mA at room temperature, using Cu Kα radiation combined with nickel filter. The diffraction angle 2θ falls between 20 and 80°.

O_2-TPD experiment was carried out on a homemade apparatus equipped with a thermal conductivity detector (TCD). The sample was first treated at 1,073 K in O_2 for 1 h and cooled to room temperature in the same atmosphere, then swept with helium at a rate of 11.8 mL/min until the baseline on the recorder remained unchanged. Finally, the sample was heated to 1,173 K at a rate of 20 K/min in helium to record the spectra.

H_2-TPR measurement was carried out on the same apparatus. After the treatment at 1,073 K in O_2 for 1 h, the sample was cooled to room temperature in the same atmosphere, and then 4.88% H_2/N_2 at a rate of 23.3 mL/min was switched on to stabilize the baseline. The sample was finally heated to 1,173 K at a rate of 20 K/min in 4.88% H_2/N_2 to record the spectra.

2.3 Catalytic Reaction

Steady-state activities of the catalysts were evaluated using a single-pass flow micro-reactor made of quartz with an internal diameter of 6 mm. In the absence of oxygen, 0.5 g catalyst is used and the reactant gas is 1.0%NO/He with a flow rate of 25 mL/min; In the presence of oxygen, 0.8 g catalyst is used and the reactant gas is (1.0%NO–2.5%O_2)/He with a flow rate of 40 mL/min. In both cases, the space velocity was kept at $W/F = 1.2$ g s mL^{-1}. The gas compositions were analyzed by an online gas chromatograph, using a molecular sieve 5A column for separating NO, N_2 and O_2. Here, N_2O is not detected since it is difficult to form between 773 and 1,123 K as reported by Teraoka et al. [10]. Before the data were obtained, reactions were maintained for a period of ~2 h at each temperature to ensure steady-state conditions. The activity was evaluated as: % (N_2 yield) = $(2[N_2]_{out}/[NO]_{in}) \times 100$, where $[NO]_{in}$ and $[N_2]_{out}$ are the inlet and outlet concentration of NO and N_2, respectively.

3 Results and Discussion

3.1 XRD

Figure 1 is the XRD patterns of $LaSrMn_{1-x}Ni_xO_{4+\delta}$ ($0.0 \leq x \leq 1.0$). For Ni-rich samples ($x = 0.5$, 0.8, and 1.0), the well-observed diffraction peaks indicate that they are typical perovskite-like oxides with A_2BO_4 structure. While for Mn-rich ones ($x = 0$ and 0.2), although the characteristic peaks belonging to oxides with A_2BO_4 structure are also observed, they are a little dispersion and some peaks indexed to Mn_2O_3 are detected. It has been reported that the preparation of pure $LaSrMnO_4$ requires rigorous conditions, such as calcination temperature at 1,773 K and calcination time of 50 h [18]. Therefore, it is acceptable that some impurities appear in $LaSrMn_{1-x}Ni_xO_{4+\delta}$ ($0 \leq x \leq 0.2$) due to the 'low' calcination temperature (1,173 K) and 'short' calcination time (6 h) used here. In this work, the influence of Mn_2O_3 could be neglected since its amount is few and its activity for NO decomposition [19] is far lower than that of the $LaSrMn_{1-x}Ni_xO_{4+\delta}$.

It should be noted that the application of citrate acid to the synthesis of mixed oxide type materials containing Sr is complex, due to the potential formation of rather stable $SrCO_3$. We previous [11] have shown that the $SrCO_3$ phase is indeed observed when scanned by IR spectrum, but it has not been detected by XRD patterns, possible reasons are

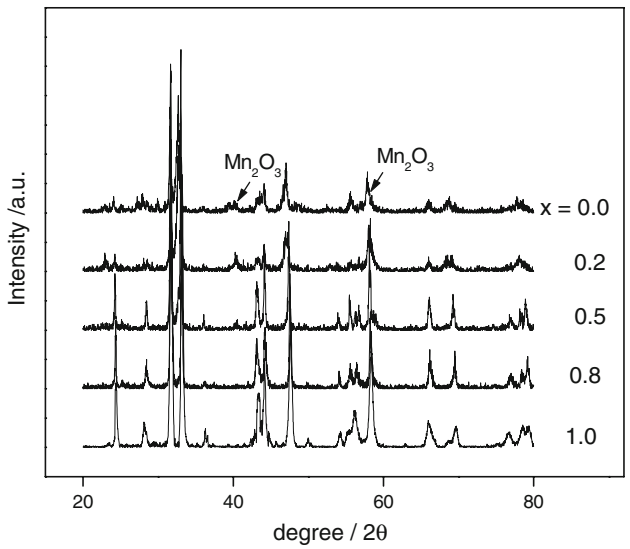

Fig. 1 XRD patterns measured from $LaSrMn_{1-x}Ni_xO_{4+\delta}$ ($0 \leq x \leq 1$)

that $SrCO_3$ is highly dispersed in the sample and its amount is few. Luckily, it seems that the $SrCO_3$ phase does not interfere with the catalytic behaviors of the catalyst. Therefore, despite of the formation of $SrCO_3$ phase, this method has been largely used in the preparation of perovskite-type mixed oxides, such as in Refs. [20–22]. In the present case, the $SrCO_3$ phase also has not been detected by XRD patterns and its influence on the reaction is neglected.

3.2 BET Surface Area

The specific surface areas of the samples are listed in Table 1. It is seen that the surface areas of all the samples are similar and range from 6 to 8 m^2/g, suggesting that the difference in the BET surface areas of the samples could be neglected at this time. This is in accordance with the results reported in ref. [23], in which it shows that the catalysts with A_2BO_4 structure prepared by combustion method and calcined at 1,173 K exhibit similar BET surface area (6–8 m^2/g). This result also suggests that the difference in activity (see Sect. 3.5) should not be ascribed to the physical factor (i.e., BET), but to the chemical nature of the catalyst, since all of them have similar BET surface area.

3.3 O_2-TPD

O_2-TPD profiles of the samples are shown in Fig. 2. In general, the oxygen desorbs from the perovskite-like mixed oxides could be differentiated into three kinds of species, namely, the ordinarily chemically adsorbed oxygen

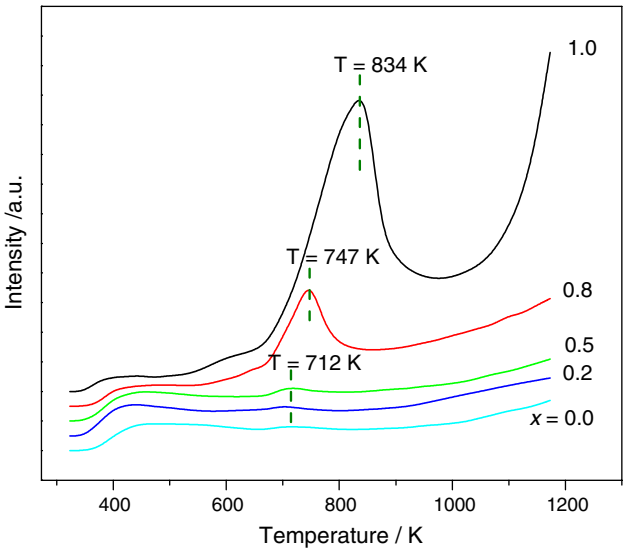

Fig. 2 O_2-TPD profiles measured from $LaSrMn_{1-x}Ni_xO_{4+\delta}$ ($0 \leq x \leq 1$)

Table 1 Data obtained from $LaSrMn_{1-x}Ni_xO_{4+\delta}$ ($0 \leq x \leq 1$)

Catalysts	BET (m^2/g)	$A_{\alpha'}$ (a.u.)[a]	A_F (a.u.)[b]	A_S (a.u.)[c]	ΔE (V)[d]	N_2 yield (%)[e]
$LaSrMnO_{4+\delta}$	6.72	8.8	239.7	71.0	0.324	27.7
$LaSrMn_{0.8}Ni_{0.2}O_{4+\delta}$	7.75	12.9	350.3	247.3	0.300	28.0
$LaSrMn_{0.5}Ni_{0.5}O_{4+\delta}$	7.48	35.0	565.8	133.0	0.377	48.1
$LaSrMn_{0.2}Ni_{0.8}O_{4+\delta}$	7.42	221.2	616.1	33.0	0.452	72.4
$LaSrNiO_{4+\delta}$	6.46	1,255.8	865.4	464.1	0.357	38.0

[a] The desorption area of α' oxygen (measured in O_2-TPD experiment)

[b] The area of the first reduction peak

[c] The area of the second reduction peak

[d] Here, the data was measured at $T = 1{,}123$ K

[e] Data measured in the presence of 2.5 v/v% O_2, $T = 1{,}123$ K

(α oxygen), the oxygen chemically adsorbed on the oxygen vacancy (α′ oxygen) and the lattice oxygen (β oxygen). According to Ref. [14], the peaks observed in the range of 323 K < T < 500 K, 573 K < T < 973 K, and T > 973 K are corresponded to α, α′ and β oxygen, respectively. No obvious difference is observed in the peak area of α and β oxygen for all the samples except $LaSrNiO_4$, of which the peak area of β oxygen increases abruptly after 1,000 K. The peak area of α′ oxygen changes regularly, in sequence of $LaSrMnO_{4+\delta} < LaSrMn_{0.8}Ni_{0.2}O_{4+\delta} < LaSrMn_{0.5}Ni_{0.5}O_{4+\delta} < LaSrMn_{0.2}Ni_{0.8}O_{4+\delta} < LaSrNiO_{4+\delta}$, indicating that higher Ni content leads to more oxygen vacancies (the relative quantities are listed in Table 1), due to its lower oxidation state (Ni^{2+}, compared with Mn^{3+}). The low peak area of α′ oxygen observed in the Mn-rich samples ($x = 0.0$ and 0.2) indicate that oxygen vacancy is difficult to be created due to the large amount of Mn, which has high oxidation state (+3). The abrupt increase of β oxygen in $LaSrNiO_{4+\delta}$ implies that the removal of lattice oxygen from $LaSrNiO_{4+\delta}$ is the easiest, that is, the structure stability of $LaSrNiO_{4+\delta}$ is far lower than that of the others, in which Mn is contained. In other words, the presence of Mn would stabilize the A_2BO_4 structure of the sample.

It has been reported that oxygen vacancy is the location of NO adsorption and dissociation, as below (here, "V_o" represents the oxygen vacancy):

$$2M^{n+} + 2V_o + 2NO \rightarrow 2\left[M^{n+1} - V_o(NO)^-\right] \rightarrow 2M^{n+1} + 2[O^-] + N_2. \quad (1)$$

After NO dissociation, the oxygen left on the surface desorbs either through the simple desorption of two vicinal oxygens [24–26] or through the decomposition of NO_3^- species [27] or both of them:

$$2M^{n+1} + 2[O^-] \rightarrow 2M^{n+} + 2V_o + O_2 \quad (2)$$

And/or

$$2M^{n+1} + 2[O^-] + NO \rightarrow 2\left[M^{n+1} - V_o(NO_3)^-\right] \rightarrow 2M^{n+} + 2V_o + O_2 + NO. \quad (2')$$

For perovskite (-like) catalysts, it is generally accepted that the oxygen vacancies are formed by charge compensation of the partial substitution of the ions as well as by thermal desorption of the oxygen at elevated temperatures. In the present case, the charge compensation originating from the partial substitution of Sr^{2+} for La^{3+} and Ni^{2+} for Mn^{3+} can be achieved by the stoichiometric formation of Ni^{3+}, Mn^{2+} and oxygen vacancy, V_o:

$$La^{3+}Sr^{2+}Mn^{3+}_{1-x-z}Mn^{2+}_{z}Ni^{2+}_{x-y}Ni^{3+}_{y}O^{2-}_{4+\delta}(V_o)^0_{\delta} \quad (\delta \geq 0). \quad (3)$$

According to the principle of electroneutrality, the following equation could be obtained:

$$3 + 2 + 3(1 - x - z) + 2z + 2(x - y) + 3y - 2(4 + \delta) = 0.$$

After simplification, the above equation could be written as:

$$2\delta = -\{(x - y) + z\}.$$

In order to create the oxygen vacancy, the value of $\{(x - y) + z\}$ should be equal to or greater than zero, that is, there at least exist some amount of metals with +2 oxidative state (Mn^{2+} and/or Ni^{2+}). This is reasonable, since the catalytic reaction requires the transformation of the metals, such as: $Ni^{2+} \Leftrightarrow Ni^{3+}$. The existence Mn^{2+} and/or Ni^{2+} ensures the creation of oxygen vacancy, which has been reported to be a crucial parameter of NO decomposition [28].

However, as shown in reactions (1) and (2) or (2), the total reaction process requires not only the presence of oxygen vacancy, but also the redox cycle of metal ions (i.e., $Mn^{2+} \Leftrightarrow Mn^{3+}$ and/or $Ni^{2+} \Leftrightarrow Ni^{3+}$), hence, we can not increase the number of oxygen vacancy unlimitedly without considering the redox behavior of the metal ions. The existence of excess oxygen vacancy would make the oxidization of the metal ions ($Mn^{2+} \rightarrow Mn^{3+}$ and/or $Ni^{2+} \rightarrow Ni^{3+}$) difficult. At present, we cannot identify directly which redox couple is responsible for the catalysis since the participation of both Mn^{2+}/Mn^{3+} and Ni^{2+}/Ni^{3+} couple is possible. However, based on the order of activity (see Sect. 3.5), it could be inferred that the Ni^{2+}/Ni^{3+} couple dominates the reaction. While the role of Mn is mainly to speed the Ni oxidization ($Ni^{2+} \rightarrow Ni^{3+}$) and to promote the NO dissociation (see reaction (1)) through reducing the number of oxygen vacancy, due to its high oxidation state. Besides, a complex active site (Mn^{2+}–(O)–(Ni^{2+}–O–Ni^{2+}) ⇔ Mn^{3+}–(O)–(Ni^{2+}–[]–Ni^{3+}) + O^{2-}) that facilitates oxygen mobility might also be formed due to the alterable valence of Mn, accelerating the regeneration of oxygen vacancy.

3.4 H_2-TPR

The results from H_2-TPR measurements are shown in Fig. 3. In general, the reduction of the perovskite (-like) mixed oxides proceeds in two steps. For $LaSrMnO_{4+\delta}$ and $LaSrNiO_{4+\delta}$, in which only one transition metal is involved, the first reduction peak of them locates at different temperature range. Based on this difference, it could be classified that the reduction peak at 823 K < T < 853 K is ascribed to the reduction of Mn^{3+}–Mn^{2+} and that at 723 K < T < 763 K is to the reduction of Ni^{3+}–Ni^{2+}. This is in accordance with the results reported by Patcas et al. [29] (see the embedded picture in Fig. 3). For $LaSrMn_{0.8}Ni_{0.2}O_{4+\delta}$, a shoulder peak at T = 753 K is observed but it is a little difficult to differentiate this

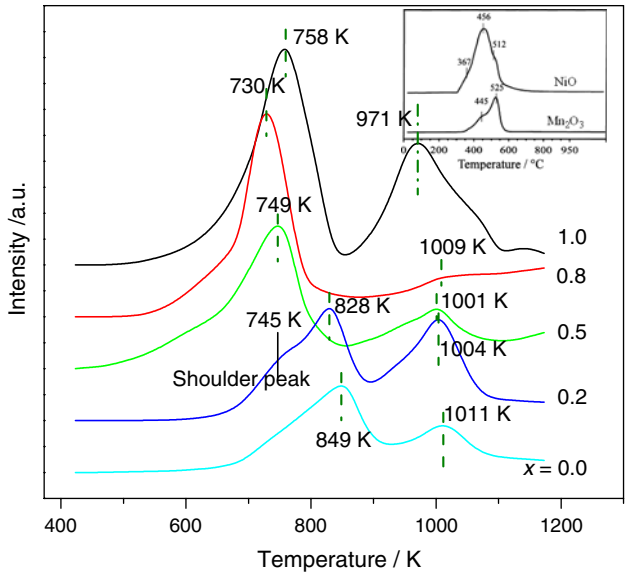

Fig. 3 TPR measurements of $LaSrMn_{1-x}Ni_xO_{4+\delta}$ ($0 \le x \le 1$)

attribution is from Mn^{3+}/Mn^{2+} or Ni^{3+}/Ni^{2+}, since a shoulder peak at a similar location is also observed for Mn_2O_3 and the Ni content is minor at this time. For $LaSrMn_{1-x}Ni_xO_{4+\delta}$ ($x = 0.5$ and 0.8), the first reduction peak locates at $723\ K < T < 763\ K$ and no shoulder peak is observed. This peak, we think, is mainly ascribed to the reduction of Ni^{3+}–Ni^{2+}, since the major reduction peak of Mn_2O_3 is not observed. In principle, these two catalysts should show two reduction peaks at $T < 853$ K corresponding to the reduction of Ni^{3+}/Ni^{2+} and Mn^{3+}/Mn^{2+}, respectively. Only one observed reduction peak indicates that manganese is mainly in Mn^{2+} form, or the reduction peak of Mn^{3+}/Mn^{2+} is too small and is overlapped by that of Ni^{3+}/Ni^{2+}. The reduction temperature of $LaSrNiO_4$ is lower than that of $LaSrMnO_4$, which suggests that the reduction of Ni^{3+}/Ni^{2+} is easier than that of Mn^{3+}/Mn^{2+}.

The second reduction peak of samples locates at a higher temperature range ($963\ K < T < 1{,}013\ K$) and is corresponding to the reduction of Mn^{2+}/Mn^0 and/or Ni^{2+}/Ni^0. The temperature of the second reduction peak, as well as that of the first one, decreases with the Ni content (except for $LaSrNiO_{4+\delta}$). But the area of the second reduction peak is complex. Although the peak area of $LaSrNiO_{4+\delta}$ is the largest, that of other samples ($0.2 < x < 0.8$) decreases with the increase of Ni content, and only a minor reduction peak is observed in $LaSrMn_{0.2}Ni_{0.8}O_{4+\delta}$. The small reduction peak indicates that the reduction of Ni^{2+}–Ni^0 in $LaSrMn_{0.2}Ni_{0.8}O_{4+\delta}$ is more difficult than that in the others. The peak area of $LaSrMnO_{4+\delta}$ is moderate in comparison to that of the others.

By plotting the temperature difference between the two reduction peaks, ΔT, as a function of the Ni content, a clear correlation is observed, as shown in Fig. 4. The value of ΔT increases from 160 to 280 K with the substitution of Ni for Mn, but then decreases to 200 K at $x = 1$. It has been reported that small temperature difference corresponds to close energies of M^{n+1}/M^{n+} and M^{n+}/M^{n-1}, and a low relative position of Fermi level [9]. Therefore, we consider that big temperature difference will correspond to large energies of M^{n+1}/M^{n+} and M^{n+}/M^{n-1}, and a high relative position of Fermi level (i.e., the system is more reducing). The Ni-rich samples ($x \ge 0.5$) are, in other word, strong reducing catalyst than the Mn-rich ones. The relationships between the activity and the Ni content are also plotted in Fig. 4. Interestingly, the trends of activity and ΔT versus Ni content are dramatically similar, suggesting that the activity of NO decomposition has a close relation to the reducibility of catalyst. As a result, we conclude that the oxidization process of catalyst, corresponding to the NO adsorption and dissociation (see reaction (1)), is the crucial step of NO decomposition in this case. This is similar to the findings reported elsewhere [30].

Also, we calculate the ratio of the first reduction peak area (A_F) to the second reduction peak area (A_S), $r = A_F/A_S$, and the results are listed in Table 1. It is seen that the change of this ratio (r) has the same trend as that of the activity, suggesting a close relationship of them. In general, there are two kinds of reacting species involved in the TPR measurement: one is the oxygen and the other is B-site cation (i.e., $H_2 + 2M^{n+1} + O^{2-} \rightarrow 2M^{n+} + H_2O$), both of which compose of the redox property of catalyst, and it is impossible to differentiate them independently. Thus, we propose to use the ratio r to represent the redox property, with a similar formulation as the Nerst Equation, as below:

$$\Delta E = (RT/nF) \cdot \ln\left\{\left(C^{n+1}/C^{n+}\right)/\left(C^{n+}/C^{n-1}\right)\right\} = (RT/nF) \cdot \ln(A_F/A_S) = (RT/nF) \cdot \ln(r)$$

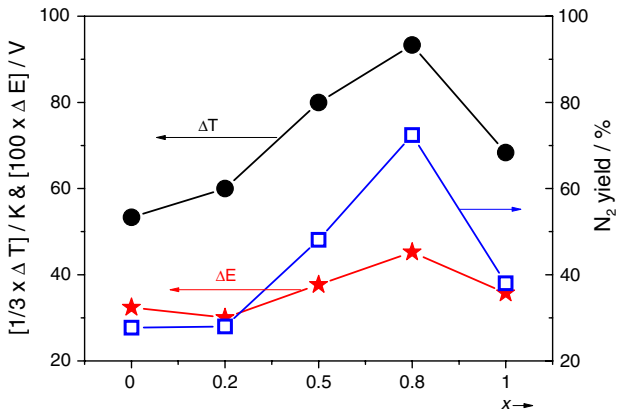

Fig. 4 Relationships between the ΔT, the ΔE, the activity (in 2.5 v/v% O_2, 1,123 K) and the Ni content of $LaSrMn_{0.2}Ni_{0.8}O_{4+\delta}$

Here, "C" represents the catalyst; it contains the transition metal and oxygen vacancy. ΔE values of the samples are calculated and listed in Table 1. Interestingly, it is also found that the ΔE has the same trend as the activity (except for $LaSrMnO_4$), as shown in Fig. 4. Recalled the relationships between ΔT and activity, it could be concluded that there should be an essential correlation between ΔT and ΔE. As discussed above, large ΔT corresponds to strong reducibility of the catalyst, namely, the easy oxidation of M^{n+}–M^{n+1}; while large ΔE corresponds to small area of the second reduction peak, namely, the difficult reduction of M^{n+}–M^{n-1}. That is to say, the increase in ΔT or ΔE is to decrease the reductive potential or to increase the oxidative potential of the catalyst, the aim of both is to decrease the difference in redox potentials, i.e., to have more matched redox potentials. This is the common ground of them. As a result, the increase of either ΔT or ΔE leads to the improvement of NO decomposition activity. This agrees well with our previous result [12], where the redox potentials of catalyst are measured by CV technique.

3.5 Catalytic Activity

Catalytic activities of the samples for NO decomposition in the absence/presence of oxygen are shown in Fig. 5 (1.0%NO/He) and Fig. 6 (1.0%NO–2.5%O_2/He). It is seen that the activity increases with the temperature and/or the Ni content (except $LaSrNiO_4$). The dependence of temperature maybe ascribed to the reason that (1) this reaction is thermodynamic favorable and (2) the regeneration of oxygen vacancy (active site) is accelerated at high temperature, improving the reaction frequency and hence the activity. The increase of activity with the Ni content might

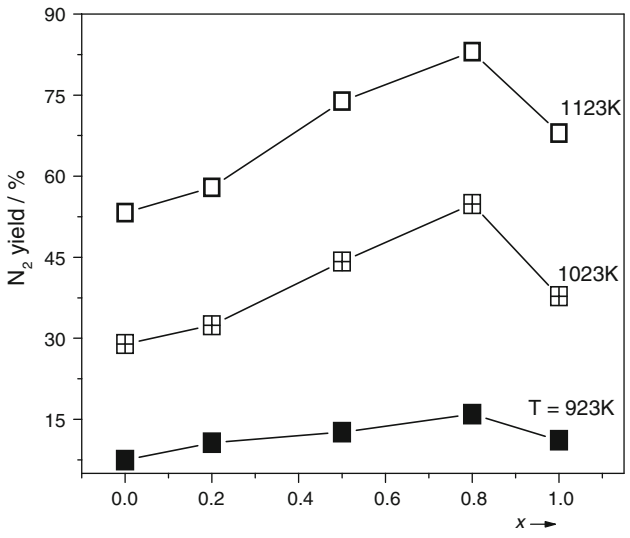

Fig. 5 Activity of NO decomposition measured over $LaSrMn_{1-x}Ni_xO_{4+\delta}$ ($0 \le x \le 1$), in the absence of oxygen

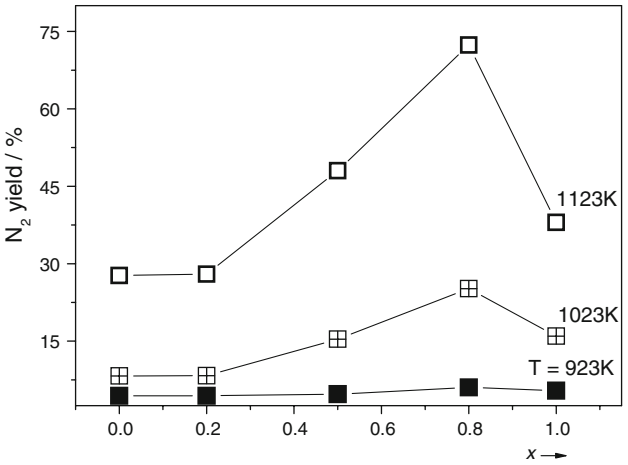

Fig. 6 Activity of NO decomposition measured over $LaSrMn_{1-x}Ni_xO_{4+\delta}$ ($0 \le x \le 1$), in the presence of 2.5v/v% O_2

be partly ascribed to the low valence of Ni (+2), which, according to the law of electroneurality, would result in the increase of oxygen vacancy that facilitates NO adsorption and dissociation. This result also suggests that Ni is a more suitable transition metal for NO decomposition than Mn, whereas a minor amount of Mn in the structure would help to improve the activity.

When oxygen is present in the feed gas, the trend of activity is similar to that in the absence of oxygen except that the activity is lower. However, it should be noted that the activity of $LaSrMn_{0.5}Ni_{0.5}O_{4+\delta}$ and $LaSrNiO_{4+\delta}$ is far lower than that of $LaSrMn_{0.2}Ni_{0.8}O_{4+\delta}$ especially at high temperatures ($T = 1{,}123$ K). The reason might be that the latter possesses larger number of oxygen vacancies (compared with $LaSrMn_{0.5}Ni_{0.5}O_{4+\delta}$, see TPD result) and at the same time, stronger reducibility (compared with $LaSrNiO_{4+\delta}$, see TPR result). Hence, the negative effect of oxygen on the catalytic performance of $LaSrMn_{0.2}Ni_{0.8}O_{4+\delta}$ is weaker than that on $LaSrMn_{0.5}Ni_{0.5}O_{4+\delta}$ or $LaSrNiO_{4+\delta}$, leading to a bigger difference in activity of them, especially at high temperature range. At low temperature ($T = 923$ K), all the catalysts exhibit low activity for NO decomposition.

For a complete catalytic reaction, it includes the oxidation and reduction steps. In case of NO direct decomposition reaction, these two steps are performed totally by the catalyst itself due to the lack of reducing agent in the feed gas. Accordingly, the catalyst is required to exhibit the ability both to oxidize and to reduce, as shown in reactions (1) and (2) or (2). Reaction (1) requires the catalyst to be oxidized ($M^{n+} \rightarrow M^{n+1}$) so that NO could be actively adsorbed on the active site, while reaction (2) or (2) requires the catalyst to be reduced ($M^{n+1} \rightarrow M^{n+}$) to impel the adsorbed oxygen leaving from the oxygen vacancy, i.e., the regeneration of the active site. Hence, the catalyst at this time should possess good ability both to oxidation and to reduction, namely,

matched redox ability. This might be the reason why $LaSrMn_{0.2}Ni_{0.8}O_{4+\delta}$, which shows the largest ΔT and ΔE value, exhibits the best NO decomposition activity.

In all, the above results indicate that NO decomposition reaction depends greatly on the redox capacity of the catalysts (which includes the redox cycle of oxygen vacancies and that of transition metals). The redox capacity of the catalyst increases strongly with the nickel content, showing a maximum at $LaSrMn_{0.2}Ni_{0.8}O_{4+\delta}$ in the present study. Inui et al. [31] also reported that a high redox capacity is necessary for achieving a high catalytic activity on metallosilicates. While for NO reduction over pervoskite [9], it is reported that the redox capacity only has a minor effect on the catalytic activity, due to the presence of reducing agent, which could compensate the reducibility of the catalyst. This difference indicates that the mechanism of NO decomposition and NO reduction is different. The catalytic activity is therefore determined by more factors.

4 Conclusion

Perovskite-like mixed oxides, $LaSrMn_{1-x}Ni_xO_{4+\delta}$ ($0.0 \leq x \leq 1.0$), have been investigated as catalysts for NO direct decomposition. Catalytic activity increases with the increase of Ni content, but then decreases when Mn is completely replaced by Ni, indicating that (1) Ni is a more active element than Mn when used for NO decomposition reaction, and (2) the existence of Mn is necessary for improving the activity. Two parameters (i.e., ΔT and ΔE) that reflect the reducibility and oxidability of catalyst are introduced in order to explain the difference in activity. It should be pointed out that the change regulation in ΔT or ΔE of $LaSrMn_{1-x}Ni_xO_{4+\delta}$ ($0.0 \leq x \leq 1.0$) sometimes cannot be applied to the extreme case ($x = 0.0$ or 1.0), in which only one transition metal (Mn or Ni) is contained. Compared with NO reduction reaction, in which a reducing agent is present and only the oxidability of catalyst is required, the NO decomposition requires the catalyst to exhibit good ability both to reduction and to oxidation, due to the absence of reducing agent.

Acknowledgments Financial support from the Ministry of science and technology of China (2001AA 324060) and the Natural science foundation of China (20177022) is greatly appreciated.

References

1. Liu J, Zhao Z, Xu CM, Duan AJ, Jiang GY (2008) J Phys Chem C 112:5930 references therein
2. Voorhoeve RJH (1977) Advanced materials in catalysis. Academic Press, New York, p 129
3. Wang H, Zhao Z, Liang P, Xu CM, Duan AJ, Jiang GY, Xu J, Liu J (2008) Catal Lett 124:91
4. Kubaschewski O, Alckock CB, Spencer PJ (1993) Materials thermochemistry, 6th edn. Pergamon Press, Oxford
5. Voorhoeve RJH (1977) Advanced materials in catalysi. Academic Press, New York, p 129
6. Mizusaki J, Mori N, Takai H, Yonemura Y, Minamiue H, Tagawa H, Dokiya M, Inaba H, Naraya K, Sasamoto T, Hashimoto T (2000) Solid State Ion 129:163
7. Tofan C, Klvana D, Kirchnerova J (2002) Appl Catal A Gen 223:275
8. Buciuman FC, Joubert E, Menezo JC, Barbier J (2001) Appl Catal A Gen 35:149
9. Hansen KK, Skou EM, Christensen H, Turek T (2000) J Catal 199:132
10. Teraoka Y, Fukada H, Kagawa S (1990) Chem Lett: 1
11. Zhu JJ, Xiao DH, Li J, Yang XG, Wu Y (2005) J Mol Catal A Chem 234:99
12. Zhu JJ, Zhao Z, Xiao DH, Li J, Yang XG, Wu Y (2005) Electrochem Commun 7:58
13. Ladavos AK, Pomonis PJ (1991) J Chem Soc Faraday Trans 87:3291
14. Zhao Z, Yang XG, Wu Y (1996) Appl Catal B Environ 8:281
15. Ladavos AK, Pomonis PJ (1997) Appl Catal A Gen 165:73
16. Zhu JJ, Xiao DH, Li J, Xie XF, Yang XG, Wu Y (2005) J Mol Catal A Chem 233:29
17. Yu ZL, Gao LZ, Yuan SY, Wu Y (1992) J Chem Soc Faraday Trans 88:3245
18. Reutler P, Friedt O, Büchner B, Braden M, Revcolevschi A (2003) J Cryst Growth 249:222
19. Yamashita T, Vannice A (1996) J Catal 163:158
20. Martynczuk J, Arnold M, Wang H, Caro J, Feldhoff A (2007) Adv Mater 19:2134
21. Białobok B, Trawczynski J, Mista W, Zawadzki M (2007) Appl Catal B Environ 72:395
22. Augustin CO, Kalai Selvan R, Nagaraj R, John Berchmans L (2005) Mater Chem Phys 89:406
23. Zhong H, Zeng R (2006) J Serb Chem Soc 71:1049
24. Shin S, Arakawa H, Hatakeyama Y, Ogawa K, Shimomura K (1979) Mat Res Bull 14:633
25. Teraoka Y, Harada T, Kagawa S (1998) J Chem Soc Faraday Trans 94:1887
26. Ishihara T, Ando M, Sada K, Takiishi K, Yamada K, Nishiguchi H, Takita Y (2003) J Catal 220:104
27. Moden B, Costa PD, Fonfe B, Lee DK, Iglesia E (2002) J Catal 209:75
28. Yokoi Y, Uchida H (1998) Catal Today 42:167
29. Patcas F, Buciuman FC, Zsako J (2000) Thermochim Acta 360:71
30. Seiyama T (1993) Properties and Applications of Perovskite-type oxides In: Tejuca LG, Fierro JLG (Eds) Marcel Dekker, New York, p 215
31. Inui T, Iwamoto S, Kojo S, Shimizu S, Hirabayashi T (1994) Catal Today 22:41